Comparison of Effectiveness and Energy Use of Airborne Pathogen Mitigation Measures to Meet Clean Air Targets in a Prototypical Office Building

Cary A. Faulkner [a], Timothy I. Salsbury [a], Belal Abboushi [a], Cerrina Mouchref [a], Brett C. Singer [b], Michael D. Sohn [b], Gabe Arnold [a]

[a] Pacific Northwest National Laboratory, 902 Batelle Blvd, Richland, 99354, WA, USA
[b] Lawrence Berkeley National Laboratory, 1 Cyclotron Road, Berkeley, 94720, CA, USA

Corresponding author: Cary A. Faulkner, cary.faulkner@pnnl.gov

This is an archival copy of an article published in *Building and Environment.* Please cite as:

Cary A. Faulkner, Timothy I. Salsbury, Belal Abboushi, Cerrina Mouchref, Brett C. Singer, Michael D. Sohn, Gabe Arnold. Comparison of Effectiveness and Energy Use of Airborne Pathogen Mitigation Measures to Meet Clean Air Targets in a Prototypical Office Building. *Building and Environment*. 257 (2024) 111466. doi.org/10.1016/j.buildenv.2024.111466

Comparison of Effectiveness and Energy Use of Airborne Pathogen Mitigation Measures to Meet Clean Air Targets in a Prototypical Office Building

Cary A. Faulkner[a], Timothy I. Salsbury[a], Belal Abboushi[a], Cerrina Mouchref[a], Brett C. Singer[b], Michael D. Sohn[b], Gabe Arnold[a]

[a] *Pacific Northwest National Laboratory, 902 Batelle Blvd, Richland, 99354, WA, U.S.A.*
[b] *Lawrence Berkeley National Laboratory, 1 Cyclotron Road, Berkeley, 94720, CA, U.S.A.*

Abstract

Organizations such as ASHRAE and the Centers for Disease Control and Prevention (CDC) have proposed guidelines for controlling infectious aerosols in buildings, which can be met through measures such as modified operation of the heating, ventilation, and air-conditioning (HVAC) system or incorporating air-cleaning technologies. However, more research is needed to understand the trade-offs between health, energy, and comfort aspects when designing measures for these guidelines. To address this gap, this paper presents an analysis using new models for air-cleaning technologies, including in-duct and in-room germicidal ultraviolet (GUV) systems and portable air cleaners (PACs). These models are incorporated into an existing prototypical office building model and six measures are designed to meet ASHRAE Standard 241 and CDC clean air targets: MERV 13 HVAC filtration, maximum outdoor air supplied to the building, PACs, and in-duct, upper-room, and whole-room GUV. The measures are simulated for an office building in a cool and humid climate compared against a baseline simulation using MERV 8 filtration. The results show that all measures, except for the maximum outdoor air case, can meet the ASHRAE 241 standard without significant impacts on energy or comfort. The HVAC system measures were not able to meet the CDC target with the default system sizing and lead to significant energy increases, while the in-room measures were able to meet the CDC target with small impacts on energy consumption. This paper consolidates the simulation findings and provides practical guidance for building operators to meet clean air targets while limiting energy and comfort impacts.

Keywords: Indoor air quality, ASHRAE Standard 241, GUV, filtration, ventilation

1. Introduction

The COVID-19 pandemic demonstrated the significant risk of infection indoors and emphasized the need to improve indoor air quality. For example, one study [1] found that all 318 identified COVID-19 outbreaks of three or more people in China occurred indoors. Another study [2] identified transmission by aerosols as the likely cause of a super spreader event from a choir rehearsal. Indoor aerosol transmission may also be the major transmission route for other viruses, such as rhinovirus (virus which causes the common cold) [3]. Beyond mortality and public health impacts, absenteeism due to COVID-19 infections has been shown to have a significant impact on education [4, 5], labor force [6, 7], and more.

Organizations have taken steps to address the spread of COVID-19 and other pathogens within indoor spaces. The Centers for Disease Control and Prevention (CDC) issued guidance on clean air targets in buildings in May of 2023 [8] and ASHRAE published a new standard for controlling infectious aerosols in buildings in June of 2023 [9]. Various measures can be taken to meet clean air targets and standards, such as increasing outdoor air ventilation, upgrading in-duct filtration, implementing germicidal ultraviolet (GUV) systems, or using portable air cleaners (PACs). These measures can be applied in the heating, ventilation, and air-conditioning (HVAC) system (e.g., HVAC filtration or in-duct GUV) or in rooms directly (e.g., in-room GUV or PACs). These measures not only impact occupant health, but also affect comfort and energy use.

Previous research has evaluated various measures to limit the risk of infection from airborne pathogens indoors. Ventilation strategies have been studied extensively in healthcare facilities [10] and classrooms [11], but energy impacts are not usually the focus of these studies. Pang et al. [12] studied how increased mechanical outdoor air ventilation affects infection risk and energy consumption for office buildings in 19 climates. The results revealed the impacts of climate on infection risk and energy consumption when increasing outdoor air ventilation. Others have compared HVAC filtration with outdoor air ventilation for airborne pathogen mitigation. For example, one study [13] evaluated the infection risks and costs for various levels of filtration and outdoor air ventilation to mitigate influenza transmission and found minimum efficiency reporting value (MERV) 13-16 filters achieved the best level of reduced infection risk per cost.

Evaluations of the recent clean air targets and standards from the CDC and ASHRAE are limited, although Zaatari et al. [14] found efficient HVAC filtration to be a more cost-effective approach than outdoor air ventilation to meet these targets. Another study [15] compared the energy costs and transmission risk impacts of a transmission-controlled ventilation strategy with in-zone filtration and far UV designed to meet ASHRAE 241, in addition to comparisons with other baseline ventilation strategies (e.g., ASHRAE 62.1 [16] minimum ventilation). They found the combination of transmission-controlled ventilation and far UV to limit infection risks with low energy costs.

Studies [17, 18, 19, 20] have demonstrated the potential of GUV technologies for inactivating airborne pathogens including SARS-CoV-2 (the virus that leads to COVID-19). Other works [21, 22] have compared GUV (either in-duct or in-room) with increased filtration, outdoor air ventilation, and PACs to minimize infection risks for various commercial building types leveraging multi-zone models. These studies highlighted the ability of in-room cleaning technologies (i.e., in-room GUV or PACs) to more effectively limit infection risks compared to in-duct treatment of air (i.e., HVAC filtration or in-duct GUV). Computational fluid dynamics (CFD) methods are often used to evaluate infection risk reduction for in-room air cleaning technologies [23, 24, 25], but are rarely used for long-term energy analyses of airborne pathogen mitigation measures due to high computational requirements.

Although significant research progress has been made in evaluating airborne pathogen mitigation measures, the following research gaps exist. First, analyses of how to meet the recent ASHRAE 241 clean air standard and CDC clean air target are limited. More research is needed on how measures such as GUV and PACs compare to filtration and outdoor air ventilation for these clean air guidelines. Additionally, further research is needed to analyze and compare multiple measures including GUV technologies in terms of impacts on occupant health, comfort, and energy consumption. Oftentimes, studies focus on either air-cleaning effectiveness or energy impacts, but do not always consider both along with other impacts such as thermal comfort [26].

This paper addresses these gaps by modeling a number of airborne pathogen mitigation measures including HVAC filtration, outdoor air ventilation, in-duct GUV, upper/whole-room GUV, and PACs designed to meet the ASHRAE 241 clean air standard and CDC clean air

target. Previous studies by the authors [27, 28, 29] developed new models for HVAC filtration and virus transmission applied to a prototypical office building using models developed in Modelica [30]. This paper expands on this work by first creating new models for in-duct GUV, in-room GUV, and PAC devices. These new models are then implemented alongside the previously developed models to assess the ability of various airborne pathogen mitigation measures to meet ASHRAE Standard 241 and CDC clean air targets. This paper assumes well-mixed zones as a computationally efficient method to assess the combination of equivalent clean air, energy, and comfort metrics for the measures.

The specific scientific contributions of this paper include: 1) creating new models for in-duct GUV, in-room GUV, and PAC devices and applying them to a model of a prototypical medium size office building; 2) implementing and simulating pathogen mitigation measures including MERV 13 HVAC filtration, maximum outdoor air ventilation, in-duct GUV, upper- and whole-room GUV, and PACs to meet ASHRAE Standard 241 and the CDC clean air target for the office building model in a cool and humid climate; 3) comprehensively analyzing the results in terms of dynamic equivalent clean airflow rates, energy consumption, carbon emissions, and thermal and humidity discomfort.

The remainder of this paper is organized as follows. First, the studied clean air guidelines and airborne pathogen mitigation measures are reviewed in Section 2. Next, the new models and their implementation are described in Section 3. Section 4 then describes the evaluation methodology including key metrics and the studied scenarios. Finally, the results are presented and discussed in Section 5 and conclusions are drawn in Section 6.

2. Summary of Clean Air Guidelines and Mitigation Measures

The clean air guidelines provided by ASHRAE Standard 241 and the CDC is reviewed first in this section. Then, common airborne pathogen mitigation measures are summarized.

2.1. Clean Air Guidelines for Airborne Pathogen Mitigation

This paper focuses on the indoor environment and specifically the mitigation of airborne pathogens, and is thus supplemental to other air quality concerns such as those related to outdoor air, as in [31]. The term pathogen is used in this paper to describe a quantity of viable viruses that can lead to infection when inhaled. This work also goes beyond

more general building ventilation standards targeted at indoor pollutants, such as ASHRAE Standard 62.1 [16]. However, the simulation scenarios described in Section 4.2 are designed to meet ASHRAE Standard 62.1 ventilation requirements as well as the considered additional guidelines. ASHRAE Standard 241 and the CDC clean air target are identified for this study and are described in the following subsections. For verbal simplicity, the term guidelines is used in this when referring to both ASHRAE Standard 241 and CDC's guidance and the term clean air target(s) is used when referring to their specific equivalent clean airflow values.

2.1.1. ASHRAE Standard 241

ASHRAE Standard 241 [9] defines minimum *equivalent* clean airflow rates per person (ECA_i) for infection risk mitigation in different space types. The standard defines the ECA_i for operation during infection risk management mode (IRMM), which may be applied when infection risk levels are higher or if policies require this operation. The IRMM design occupancy may also be different than typical occupancy when IRMM is implemented. Equivalent clean airflow can be achieved through a variety of methods, including outdoor air ventilation, HVAC filtration, or air-cleaning technologies (e.g., GUV or PACs). The ECA_i is defined in terms of airflow per occupants (e.g., $L/s/person$), so the IRMM design occupancy is important in calculating the target equivalent clean airflow rate. The calculation of equivalent clean airflow for different measures is detailed in Section 4.1.1.

2.1.2. CDC Target

The CDC recommends at least five equivalent clean air changes per hour (eACH) for occupied spaces in buildings [8] and does not specify targets for different space types, other than supplemental ventilation requirements for health-care facilities [32]. The CDC acknowledges large volume spaces with few occupants (e.g., warehouses) may not need 5 eACH and spaces with high occupancy or high-risk occupants may require more than 5 eACH [8]. Similar to ASHRAE Standard 241, the clean air changes can be achieved through combinations of outdoor air ventilation, HVAC filtration, and air treatment. Unlike ASHRAE Standard 241, the clean air target is not dependent on occupancy, but rather the volume of the room. For example, multiplying five eACH by the volume of the room gives the (volumetric) clean airflow rate needed for that specific room.

2.1.3. Comparison of ASHRAE Standard 241 and CDC Targets

Table 1 compares the levels of eACH among ASHRAE 62.1, ASHRAE 241, and the CDC target for a selection of space types. This table is calculated assuming 93 m^2 (1,000 ft^2) rooms with 2.4 m (8 ft) ceiling heights and ASHRAE 62.1 design occupancy levels. The ASHRAE 62.1 eACH is calculated based on the outdoor air ventilation standards per floor area and number of occupants for these spaces. The ASHRAE 241 eACH is calculated using the defined ECA_i for these space types (listed in the table as well) and design occupancy values. Depending on the space type shown in Table 1, the eACH can increase by up to six times for ASHRAE 241 compared to ASHRAE 62.1 and up to eight times for CDC compared to ASHRAE 62.1. The CDC target may be higher or lower than ASHRAE 241 depending on the space type, room dimensions, and IRMM design occupancy.

Table 1: Example comparison of eACH levels among ASHRAE Standard 62.1, ASHRAE Standard 241, and the CDC target.

Space Type	*ASHRAE 62.1*	*ASHRAE 241*	*CDC*
Office	0.6 eACH	1.1 eACH (15 $L/s/person$)	5 eACH
Classroom	2.8 eACH	7.5 eACH (20 $L/s/person$)	5 eACH
Restaurant dining	5.3 eACH	31.5 eACH (30 $L/s/person$)	5 eACH

2.2. Airborne Pathogen Mitigation Measures

This section describes the airborne pathogen mitigation measures. Figure 1 presents an overview of many airborne pathogen mitigation measures to reduce transmission. Some of the measures are related to the operation of the HVAC system, for example increasing outdoor air ventilation or total air change rate. Others include treatment of the supply air in the HVAC system, such as using HVAC filtration or in-duct GUV. Another approach is to use air-cleaning technologies in the room, for example adding upper/whole-room GUV or PACs. The measures are categorized as HVAC system measures or in-room measures and described in more detail in the following subsections.

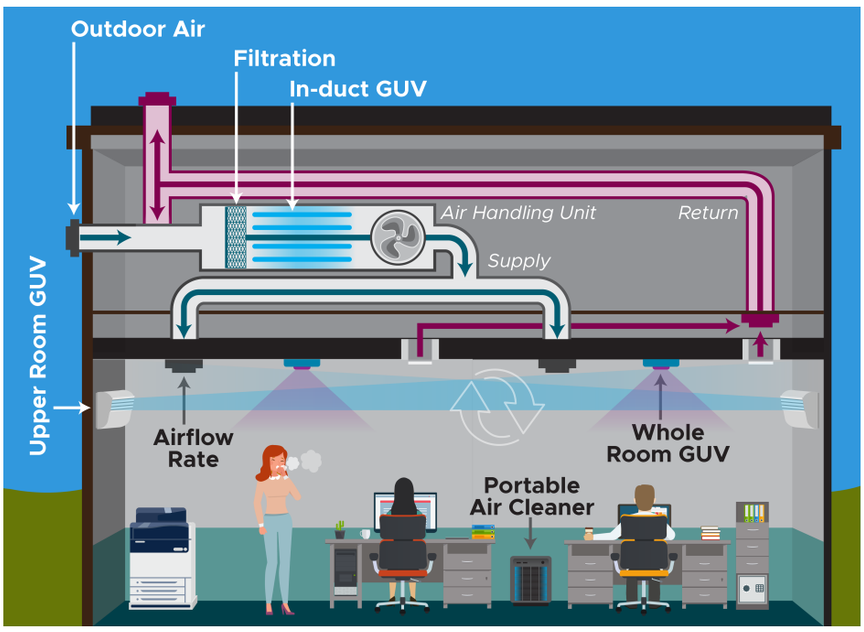

Figure 1: Schematic of mitigation measures.

2.2.1. HVAC System Measures

The first HVAC system measure is increasing outdoor air ventilation. Increasing the fraction of outdoor air in the supply air relative to recirculated air can mitigate the build-up of indoor airborne pathogens by exhausting them more quickly to the ambient environment and diluting rooms with pathogen-free outdoor air. However, this strategy can lead to increased HVAC system power to condition the outdoor air and potential introduction of more outdoor air contaminants to the indoor environment. This can also lead to thermal comfort issues if the system is not sized to account for the increased outdoor airflow.

Increasing the zone total airflow setpoint can flush pathogens out of the room faster and exhaust them to the ambient environment or recirculate them to be treated in the HVAC system. This can be accomplished for a variable-air-volume (VAV) system by increasing the minimum airflow setpoints for the zones. These minimum setpoints can potentially be increased from the ASHRAE 62.1 minimum ventilation setpoint [16] up to the maximum zone airflow setpoint based on system sizing. Raising the airflow setpoint can, however, increase fan energy consumption or displace pathogens to neighboring zones within the building [33].

HVAC filtration is another measure, which can remove pathogens that have been recirculated through the HVAC system into the supply airflow from the zones. There are different levels of filtration, often defined by a MERV rating (ranging from 1-16) or very efficient filters certified as high-efficiency particulate air filters (HEPA) [34]. Higher rated filters are designed to

capture smaller particles more efficiently, but can also impose a greater resistance (pressure drop) on the HVAC system airflow. Although, a higher MERV rating does not always result in an increased pressure drop, especially for filters below MERV 12 ratings [35]. The increased resistance can lead to higher fan energy use or lower airflow rates, especially if the system is not sized for a more efficient filter with a higher pressure drop. ASHRAE Standard 241 estimates the efficiency values of various filters considering the distribution of airborne pathogen particle sizes. These efficiencies can be used to calculate ECA_i for different filters to meet the standard.

The last HVAC system measure is use of in-duct GUV irradiation to inactivate aerosolized pathogens in the supply airflow. This technology can treat the supply airflow with little additional pressure drop in the HVAC system, compared to fibrous filters [36]. However, unlike filtration, it is used for inactivating biological contaminants and does not reduce the concentration of pollutants such as $PM_{2.5}$. Its effectiveness is also dependent on the dose of irradiation received by the pathogens, which is dependent on the supply airflow rate.

2.2.2. In-room Measures

Air-cleaning measures can also be applied in rooms directly, such as through use of GUV technology. Upper-room and whole-room GUV systems are used to inactivate aerosolized pathogens within rooms. Upper-room GUV typically uses higher wavelength (e.g., 254 nm) UV-C radiation only in the upper portions of the room, since this wavelength of energy is less safe compared to 222 nm radiation to direct at occupants. In contrast to 222 nm radiation, higher doses of irradiation can be used in the upper-room since it is not directed towards occupants. Whole-room GUV uses lower wavelength (e.g., 222 nm) UV-C radiation mounted on ceilings or upper walls and directed downward to disinfect air in the occupied zone. Lower wavelengths of UV-C have higher threshold limit values (TLVs) specified by ACGIH than 254 nm, and therefore are safe to be directed at occupants if ACGIH TLVs are not exceeded in occupied zones.

The GUV systems typically do not consume a significant amount of energy, for example 30-72 W per fixture [37, 38, 39]. Considerations of the GUV strategies include initials costs to design and implement these systems and potential concerns of secondary chemistry effects resulting in indoor volatile organic compounds and secondary organic aerosols [40]. The

effectiveness of upper-room GUV may also be particularly sensitive to the air mixing and distribution of pathogens in the rooms [41, 42, 43], since it only disinfects the upper portion of the room.

The other common in-room measure is use of PACs. PACs intake air within the room, pass the air through a filter and/or GUV radiation, then exhaust the air back into the room. They can be placed on a floor/surface or mounted to a wall/ceiling. These devices consume a small amount of energy, for example 23-87 W [44, 45]. Important considerations of PACs include noise, drafts, and recapture of just processed air (short-circuiting), especially when designed to produce high levels of clean air relative to room volume [46, 47]. PACs are also subject to being turned off, operated at lower settings, or unplugged by occupants. Lastly, the location of the PAC is also important to its effectiveness, which depends on the ventilation design and source location of contaminants [25].

3. Model Implementation

The implementation of models used for the simulation analysis in this study are detailed in this section. First, new models for air-cleaning technologies are introduced. These models facilitate analyses for comparing the effectiveness and energy use of air-cleaning devices with other measures such as filtration and ventilation. Then, a previously developed model for HVAC filtration is described. All of these models are developed in Modelica language [30] using the Modelica *Buildings* library [48, 49].

3.1. New Models for Air-cleaning Technologies

3.1.1. Portable Air Cleaners

First, the modeled filtration of airborne pathogens from PACs is described by Equation 1:

$$\dot{C}_{PAC} = \eta_{PAC} \dot{V}_{PAC} c_{zone}, \tag{1}$$

where $\dot{C}_{PAC}$ is the rate of pathogen removal by the PAC, η_{PAC} is the pathogen removal efficiency of the PAC, $\dot{V}_{PAC}$ is the volumetric airflow rate of the PAC, and c_{zone} is the pathogen concentration in the zone where the PAC is located. The pathogen concentration is denoted as c while the total quantity of pathogens is C in this paper. In this study, the

PAC airflow rates are constant when the device is on during the simulation. The PACs are also modeled to consume energy using a constant power rating and heat is dissipated into the zone by the PAC based on the consumed power. A switch is included in the model to turn the PAC on or off (i.e., the airflow and power are zero when the device is off). This model also assumes well-mixed zones with uniform concentrations. A verification of the model compared to an analytical solution of a case with PAC(s) in an empty room is included in Appendix A.

3.1.2. In-room GUV

Next, inactivation of airborne pathogens by either upper- or whole-room GUV devices is described by Equation 2:

$$\dot{C}_{GUV} = E_{avg} k_{rad} f_{rad} V_{zone} c_{zone}, \tag{2}$$

where $\dot{C}_{GUV}$ is the inactivation rate of airborne pathogens by the GUV device, E_{avg} is the average fluence rate of the GUV device (in units of power per area), k_{rad} is the susceptibility of the pathogens to the GUV irradiation (in units of area per energy), f_{rad} is the fraction of irradiated volume in the zone, and V_{zone} is the total volume of the zone. This equation is often used for modeling the inactivation of pathogens in well-mixed zones using GUV [41, 39, 42]. The parameters E_{avg}, k_{rad}, and f_{rad} are constant for a given simulation in this study (when the device is on). Similar to the PAC, the GUV devices consume energy based on a constant power rating, which is ultimately dissipated into the zone as heat. Also, a switch is implemented to turn the GUV device on or off.

3.1.3. In-duct GUV

Finally, inactivation of airborne pathogens in the supply air using in-duct GUV devices is described by Equation 3:

$$c_{out} = [1 - \eta_{GUV}(\dot{V}_{GUV})] c_{in}, \tag{3}$$

where c_{out} is the pathogen concentration exiting the flow past the device, $\eta_{GUV}(\dot{V}_{GUV})$ is the pathogen inactivation of the GUV device as a function of the flow rate, and c_{in} is the

pathogen concentration in the flow entering the irradiated space of the device. The pathogen inactivation efficiency as a function of flow rate is modeled based on the dose of GUV [39, 50]:

$$\eta_{GUV}(\dot{V}_{GUV}) = 1 - exp(-E_{avg}k_{rad}V_{rad}/\dot{V}_{GUV}), \tag{4}$$

where V_{rad} is a the volume of irradiated space in the duct. This equation is then simplified by combining terms into fewer model parameters:

$$\eta_{GUV}(\dot{V}_{GUV}) = 1 - exp(-k_{GUV}\dot{V}_{nom}/\dot{V}_{GUV}), \tag{5}$$

where k_{GUV} is a dimensionless combination of the parameters from Equation 4 and $\dot{V}_{nom}$ is the nominal flow rate of the system. This enables the efficiency to be determined by the ratio of the nominal system flow rate ($\dot{V}_{nom}$) to the simulated dynamic flow rate through the irradiated space ($\dot{V}_{GUV}$) and one additional parameter describing the rate of the irradiated dose (k_{GUV}). The parameter k_{GUV} is determined algebraically as $E_{avg}k_{rad}V_{rad}/\dot{V}_{nom}$ and is unitless.

Similar to the previous models, the in-duct GUV consumes energy based on a constant power rating, which is dissipated into the airflow as heat, and a switch is implemented to turn the device on or off. The pressure drop the device imposes on the system airflow is modeled using the same method as the HVAC filter (described in the next section), although it typically imposes a much smaller pressure drop compared to an HVAC filter. A demonstration of the model is included in Appendix A.

3.2. HVAC Filtration

A previously developed HVAC filtration model [27] is applied for this work. The filtration is modeled similar to the in-duct GUV:

$$c_{out} = (1 - \eta_{filter})c_{in}, \tag{6}$$

where c_{out} and c_{in} are the pathogen concentration in the airflow exiting and entering the filter, respectively, and η_{filter} is the filter efficiency. Unlike the in-duct GUV device, the filtration efficiency is not a function of the flow rate and the filter does not directly consume any power. However, the filter imposes a significant pressure drop on the system airflow.

This pressure drop is calculated as the product of a constant and the square of the system airflow rate. The constant is determined based on the nominal settings for the filter, for example an efficient filter with a higher pressure drop has a higher value for the constant in this equation. More about the HVAC filter model is described in [27].

4. Evaluation Methodology

This section describes the evaluation methodology. First, relevant evaluation metrics are detailed. Then, the studied simulation scenarios are summarized.

4.1. Evaluation Metrics

4.1.1. Clean Air Metrics

The clean air metrics in this study are described in this section using equivalent clean air changes per hour (eACH). The contributions of eACH from the HVAC system and in-room devices are calculated separately before being combined to determine the total eACH. First, the eACH from the HVAC system is computed as:

$$eACH_{HVAC} = [1 - (1 - f_{OA})(1 - \eta_{filter})(1 - \eta_{GUV})]\dot{V}_{zone}/V_{zone}, \tag{7}$$

where $eACH_{HVAC}$ is the eACH from the HVAC system, f_{OA} is outdoor air fraction in the supply airflow, and $\dot{V}_{zone}$ is the airflow rate supplied to the zone. This calculation is consistent with the method for determining equivalent clean airflow from in-duct air cleaning systems provided in ASHRAE Standard 241. This accounts for dilution, filtration, and/or disinfection of the supplied air by the outdoor air, HVAC filter, and/or in-duct GUV. Furthermore, if any of f_{OA}, η_{filter}, or η_{GUV} are equal to one or 100%, then the other two values do not impact the calculation as the zone airflow is already pathogen free. Only increasing the airflow rate supplied to the zone can increase $eACH_{HVAC}$ in this scenario. Also, the eACH becomes zero when all of f_{OA}, η_{filter}, or η_{GUV} are zero, since the supplied airflow is not cleaned at all.

ASHRAE Standard 241 determines the equivalent clean airflow from in-room air cleaning systems using only mechanical fibrous filters based on a weighted-average of clean air delivery rates (CADRs) for tobacco smoke, dust, and pollen. CADR for PACs using mechanical fibrous filters can be calculated as:

$$CADR_{PAC} = \eta_{filter}\dot{V}_{PAC}. \tag{8}$$

The eACH contribution from the PACs ($eACH_{PAC}$) in this study is calculated based on the $CADR_{PAC}$ (as determined based on ASHRAE Standard 241) and the volume of the zone, as described in Equation 9.

$$eACH_{PAC} = CADR_{PAC}/V_{zone}, \tag{9}$$

Lastly, the contribution of eACH from the in-room GUV devices is determined based on the model parameters used to determine pathogen inactivation, as shown in Equation 10.

$$eACH_{GUV} = f_{rad}E_{avg}k_{rad}. \tag{10}$$

The total eACH from the HVAC and in-room devices, $eACH_{tot}$, is calculated as described in Equation 11. It should be noted this does not account for any potential interference or redundancy among the methods of pathogen removal.

$$eACH_{tot} = eACH_{HVAC} + eACH_{PAC} + eACH_{GUV}. \tag{11}$$

4.1.2. Energy and Emission Metrics

Next, the energy-based metrics are described in this section. Energy metrics are an important secondary consideration for comparing measures that improve IAQ and do not introduce additional discomfort indoors. First, the energy consumption for the scenarios is calculated as:

$$E_{tot} = E_{heating} + E_{cooling} + E_{fan} + E_{device}, \tag{12}$$

where E_{tot}, $E_{heating}$, $E_{cooling}$, E_{fan}, and E_{device} are the total, heating, cooling, fan, and device energy consumption. The device energy consumption accounts for the energy consumed by the GUV or PAC devices.

The energy per clean air change can be calculated based on the total energy consumption and total eACH according to Equation 13. Similarly, Equation 14 computes the incremental

increase in energy consumption per increase in eACH for a specific measure (i) compared to the baseline simulation.

$$E/eACH = E_{tot}/eACH_{tot}. \tag{13}$$

$$\Delta E/\Delta eACH = \frac{E_{tot,i} - E_{tot,base}}{eACH_{tot,i} - eACH_{tot,base}}. \tag{14}$$

The CO_2 emissions are calculated using hourly emission factor data from the Cambium project [51]. The emission factor data varies during the day and throughout the year depending on the electricity sources used in the studied region. The hourly CO_2 emissions are determined by multiplying the hourly energy consumption by the hourly emission factor. More about calculating the CO_2 emissions can be found in [28].

4.1.3. Discomfort Metrics

Next, the discomfort metrics are described. Indoor temperature and humidity discomfort is a primary consideration for the measures since maintaining occupant comfort is critical. First, thermal discomfort in a zone is computed as the integral of the deviation below the heating setpoint or above the cooling setpoint during occupied hours:

$$T_{dis} = \int [\max(T_{zone}(t) - T_{coo,set}, 0) + \max(T_{hea,set} - T_{zone}(t), 0)]dt, \tag{15}$$

where T_{dis} is the thermal discomfort, T_{zone} is the zone temperature, $T_{coo,set}$ is the cooling setpoint temperature, and $T_{hea,set}$ is the heating setpoint temperature. This metric describes the magnitude of temperature discomfort over time by accounting for discomfort during both heating and cooling scenarios and has been used in previous studies evaluating building controls [52, 53].

Humidity discomfort is proposed as a new metric to quantify excessive humidity in a zone and is calculated similarly as thermal discomfort. According to ASHRAE 62.1 [16], the dew point shall not exceed 15 °C, so humidity discomfort is calculated as:

$$Hum_{dis} = \int \max(T_{dp,zone}(t) - 15°C, 0)dt, \tag{16}$$

where Hum_{dis} is the humidity discomfort and $T_{dp,zone}$ is the zone dew point temperature.

4.2. Simulation Scenarios

4.2.1. Prototypical Office Building System Model

The mitigation measures are studied for the middle floor of a prototypical five-zone, medium-sized office building located in Chicago, IL (cool and humid climate, ASHRAE climate zone 5A) based on the United States Department of Energy prototype [54]. The floor layout and system schematic for this building are shown in Figure 2. The floor has one core zone and four perimeter zones with ceiling heights of 2.74 m and a total floor area of 1,664 m^2. The area of the core zone is 985 m^2 and the area of the perimeter zones is 679 m^2. The system model is based on a prototype from the Modelica *Buildings* library [55].

The floor is serviced by a VAV system with one central AHU, which includes a heating coil, cooling coil, supply fan, and HVAC filter. The in-duct GUV is added to the AHU for those scenarios as well. Each zone has a VAV terminal box equipped with reheat coils and dampers to control the zone airflow. An economizer is used to control the amount of outdoor airflow and use free-cooling when advantageous. Cooling is provided via a chilled water plant with an assumed COP of 5 and heating is provided via a gas-powered hot water plant with an assumed efficiency of 0.8. The system is sized using design loads, design occupancy, and ASHRAE Standard 62.1 ventilation requirements [16]. The fan is also sized based on the system pressure drops assuming a MERV 8 filter. The system sizing is the same for all cases, since re-designing an existing HVAC system is often infeasible. Each zone is assumed to be instantaneously and perfectly well-mixed (i.e., the temperature and concentration is uniform in each zone).

Additional changes to the baseline system model are described below. First, the static pressure reset control in the AHU was replaced with a constant static pressure setpoint of 250 Pa (1 inch of water). This was done to simplify the controls, especially since no other reset controls (e.g., supply air temperature reset) are used for the system, and allow for more control over the airflow rates to meet the clean air targets in the evaluation. The HVAC system was also modified to run the system 24/7 to prevent the excessive humidity in the zones during unoccupied hours for this climate, especially during the summer. This is accomplished by running the HVAC system during unoccupied hours and resetting the heating setpoint from 20 °C to 12 °C and controlling the cooling coil to ensure the relative

humidity of the return airflow does not exceed 60%.

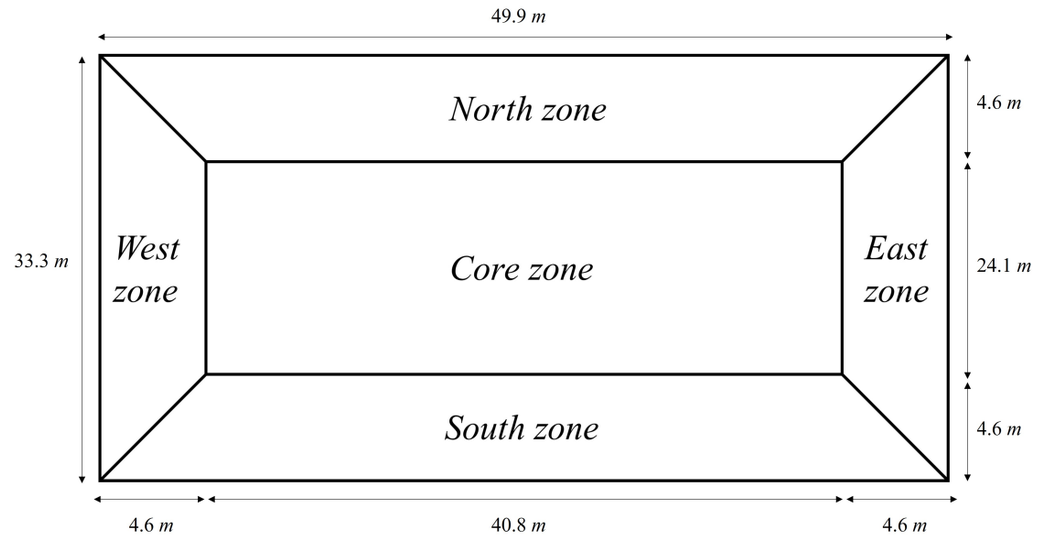

(a) Layout of the studied floor.

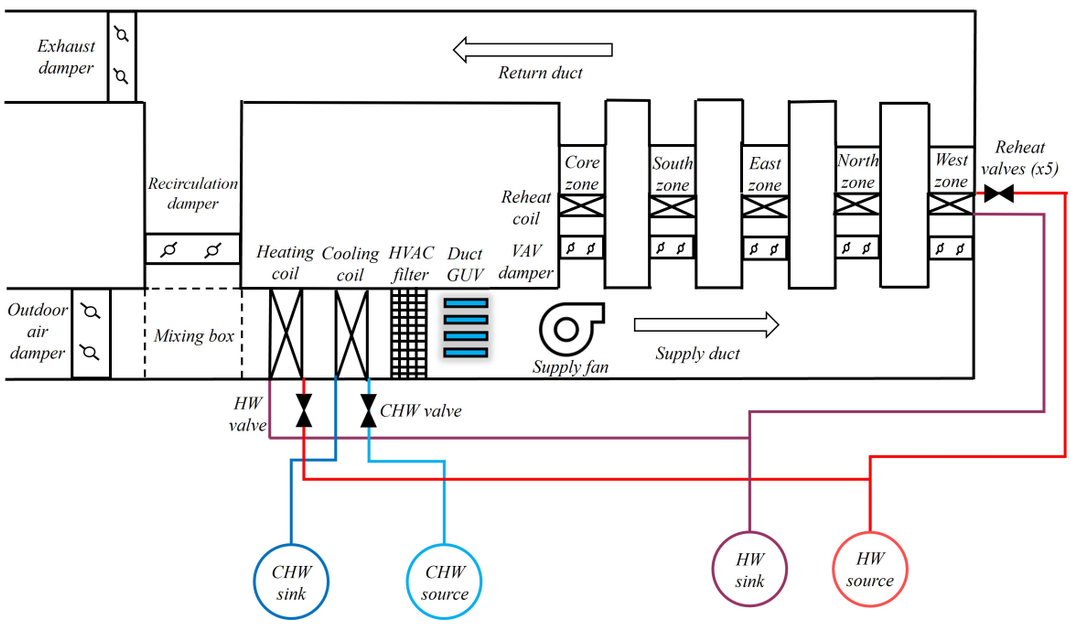

(b) System schematic.

Figure 2: Floor layout and system schematic for the prototypical five zone medium office building system.

4.2.2. Design of Measures to Meet Clean Air Targets

The studied mitigation measures are designed to meet the ASHRAE 241 and CDC clean air targets for this office building. Simulations are conducted assuming IRMM operation (i.e., operated to meet the clean air targets) for an entire year, but the results are analyzed for various temporal scales in Section 5. A baseline case that does not include IRMM operation and is not designed to meet either of the clean air targets is also included for comparison. This case uses MERV 8 filtration without any additional measures and only provides eACH via baseline outdoor airflow. Relevant parameters for the baseline and

mitigation measures in the simulations scenarios are summarized for the ASHRAE 241 cases in Table 2 and the CDC cases in 3. Many of the parameters remain the same between the ASHRAE 241 and CDC scenarios, while others are designed differently between the two sets of scenarios. Additionally, SARS-CoV-2 (the virus that leads to COVID-19) is chosen as the studied pathogen in this paper and many of the parameter values are specific to this pathogen. Although ASHRAE Standard 241 specifies using Bacteriophage MS2 as the challenge organism for testing procedures (because it is a relatively safe infectious pathogen), this study uses SARS-CoV-2 as a more representative infectious pathogen for indoor transmission scenarios. Additionally, the experimental design in this paper can be applied to study other pathogens by changing the pathogen-specific parameter values.

The following parameters are held constant for their relevant measures between the two sets of scenarios. The filtration efficiencies for MERV 8 and MERV 13 filters in this study use the recommended values from ASHRAE Standard 241. This assumes the following weighted distribution of diameters for the aerosolized pathogens: 30% 0.3-1 μm, 30% 1-3 μm, and 40% 3-10 μm. The majority of the analysis uses the recommended value of 0% filtration efficiency for MERV 8 filters by ASHRAE Standard 241, but certain results are included using an MERV 8 efficiency value of 34%, which is determined using the weighted distribution above and values from ASHRAE 52.2 [56]. The nominal pressure drop values for the filters are estimated based on the nominal (maximum) system flow rate and the average of the initial and final pressure drops. Using data for MERV 8 [57] and MERV 13 [58] filters, the recommended final pressure drop is 249 Pa (1" $w.c.$) for both filters and the estimated initial pressure drop is 95 Pa (0.38" $w.c.$) and 124 Pa (0.5" $w.c.$). The simulated pressure drop across the filters are determined as a quadratic relationship between pressure drop and flow rate based on the nominal settings, as described in Section 3.2.

The parameter k_{GUV} for the in-duct GUV cases is estimated based on data in [50, 21] and gives an inactivation efficiency of 88% at half of the nominal system flow rate. The power rating of the in-duct GUV is estimated to be 200 W for this system [59]. The pathogen susceptibility to GUV is estimated assuming radiation of wavelength 222 nm for the whole-room (WR) GUV and 254 nm for upper-room (UR) and in-duct GUV from [19]. The fraction of irradiated space, which is the volume encompassing the averaged GUV intensity,

is assumed to be 20% of the volume for UR GUV and 100% of the room for WR GUV. Since the ceiling heights are 2.74 m (9 ft) in this study, then the UR GUV fraction of irradiated space starts at 2.2 m (7.2 ft). The PACs are modeled with HEPA filters using a removal efficiency value of 99% from ASHRAE Standard 241.

Next, either the system operation or design of specific measures changes between the ASHRAE 241 and CDC scenarios. As noted in Section 2, the CDC clean air target is higher than the ASHRAE 241 standard for office buildings. This is the case in this study as the zones have a target eACH of 0.93 for the ASHRAE 241 cases (based on design occupancy) and 5 eACH for the CDC cases. The target eACH is the same for all zones for the ASHRAE 241 cases because the zones are the same space types (offices) with the same design occupant density values (0.05 occupants per m^2) and the same ratio of floor area to total volume (i.e., same ceiling heights).

The HVAC system measures including MERV 13, maximum outdoor air (referred to as max OA for the remainder of this paper), and duct GUV are implemented without any other changes to the operation for the ASHRAE 241 cases, since they are found to be sufficient by themselves to meet the standard. The exception is for the max OA case, which sometimes has an outdoor air fraction below 100% due to the controls overriding the dampers to prevent freezing of the coils or discomfort in the zones. This is done by using controls for the outdoor airflow to prevent the mixed air from dropping below 4 °C and ensuring the return temperature does not exceed the cooling setpoint (unless this occurs when the minimum outdoor airflow according to ASHRAE 62.1 is provided). Otherwise, the fraction of outdoor air is 100% during occupied hours for the max OA case. However, the implementation of the HVAC system measures alone is not sufficient to meet the CDC clean air target. This is because the total airflow rates to the zones is insufficient to meet the target, even when the supply airflow is treated or mostly outdoor air. To account for this, the zone airflow setpoints are set to their maximum values based on the default system sizing (for both heating and cooling operation) to provide enough clean airflow to the zones to meet the CDC target.

Lastly, the in-room measure cases including UR GUV, WR GUV, and PAC are calculated to meet the clean air targets using Equations 7-11. Since the HVAC system measures provide clean airflow for all the zones, the in-room measures are implemented in all the zones.

However, the parameters for the UR/WR GUV and PAC cases included in Tables 2 and 3 refer to the parameters used in the South zone, which is selected as a focus for the analysis. Many parameters are the same or similar in all the zones because of their equal values of occupant density, eACH targets, etc. For example, E_{avg} is similar in value for all the zones for a given case. While the PAC flow rate and power rating is different among the zones, normalizing those values by the zone floor area results in similar values across the zones.

A "worst case outdoor air fraction scenario" based on the minimum outdoor airflow and maximum total airflow (i.e., lowest f_{OA}) is used to determine the minimum $eACH_{HVAC}$. Then, the GUV or PACs are designed to achieve the remainder of the eACH targets. For the UR/WR GUV cases, this is done by determining how much average fluence (E_{avg}) is needed, while holding the parameters f_{rad} and k_{rad} constant. The average fluence also impacts the GUV power rating by using an estimated efficiency of 3% [39]. The occupant exposure to 222 nm UV-C light for the WR GUV cases does not exceed safety standards described in [60]. In fact, the values of E_{avg} are lower than typical design values for UR/WR GUV, for example UR GUV may have E_{avg} values in the range of 30-50 $\mu W/cm^2$ [37]. The PAC flow rate is adjusted to meet the eACH targets for the PAC cases, while holding the PAC filter efficiency constant. An assumed fan efficiency of 80% and pressure drop of 400 Pa [61] is used to correlate the PAC flow rate and power rating. The total PAC flow rate in the South zone for the CDC case corresponds to about 7 PACs with individual airflows around 400 m^3/hr over a floor area of 208 m^2, which is about one PAC per 30 m^2 (320 ft^2).

Table 2: Simulation scenarios for the ASHRAE 241 cases.

Mitigation measure	*Relevant parameters or description*
MERV 8 (Baseline)	$\eta_{filter} = 0\%$ [9]; $\Delta p_{filter} = 172\ Pa$ [57]
MERV 13	$\eta_{filter} = 77\%$ [9]; $\Delta p_{filter} = 187\ Pa$ [58]
Max OA	f_{OA} is targeted at 100%
Duct GUV	$k_{GUV} = 1.09$; $P_{GUV} = 200\ W$ [59]
UR GUV	$f_{rad} = 20\%$; $k_{rad} = 2.8\ cm^2/mJ$ [19]; $E_{avg} = 0.39\ \mu W/cm^2$; $P_{GUV} = 3.6\ W$
WR GUV	$f_{rad} = 100\%$; $k_{rad} = 3.8\ cm^2/mJ$ [19]; $E_{avg} = 0.058\ \mu W/cm^2$; $P_{GUV} = 4\ W$
PAC	$\eta_{PAC} = 99.97\%$ [62]; $\dot{V}_{PAC} = 448\ m^3/hr$; $P_{PAC} = 62\ W$

Table 3: Simulation scenarios for the CDC cases.

Mitigation measure	*Relevant parameters or description*
MERV 8 (Baseline)	$\eta_{filter} = 0\%$ [9]; $\Delta p_{filter} = 172\ Pa$ [57]
MERV 13	$\eta_{filter} = 77\%$ [9]; $\Delta p_{filter} = 187\ Pa$ [58]; zone airflow setpoints are at maximum
Max OA	f_{OA} is targeted at 100%; zone airflow setpoints are at maximum
Duct GUV	$k_{GUV} = 1.09$; $P_{GUV} = 200\ W$ [59]; zone airflow setpoints are at maximum
UR GUV	$f_{rad} = 20\%$; $k_{rad} = 2.8\ cm^2/mJ$ [19]; $E_{avg} = 2.4\ \mu W/cm^2$; $P_{GUV} = 22\ W$
WR GUV	$f_{rad} = 100\%$; $k_{rad} = 3.8\ cm^2/mJ$ [19]; $E_{avg} = 0.35\ \mu W/cm^2$; $P_{GUV} = 25\ W$
PAC	$\eta_{PAC} = 99.97\%$ [62]; $\dot{V}_{PAC} = 2,765\ m^3/hr$; $P_{PAC} = 384\ W$

5. Results and Discussion

The results of the simulations are presented and discussed in this section. First, an overview of the results at annual or monthly scales is provided. This includes eACH, energy-based, and discomfort results. Next, sample day results are analyzed in detail.

5.1. Overview of Results

5.1.1. eACH Results

Figure 3 shows violin plots representing the hourly distribution throughout the year of eACH for the various measures to meet the clean air targets. It should be noted that, although the occupancy varies during each day, the ASHRAE 241 minimum is calculated based on the design occupancy since it is assumed that the system does not know the number of occupants at each time. The eACH values are shown for the South zone and the darker horizontal bars represent the median values. The shapes of the distribution are dependent on the dynamic outdoor and total airflows at the AHU as well as the dynamic airflow supplied to the zone. Additionally, the dynamic duct GUV efficiency based on the AHU airflow rate impacts the eACH for the duct GUV cases.

Many of the distributions appear to be bimodal with two peaks corresponding to differences in operation based on season. This distribution is a result of the outdoor air usage for the in-room measures and baseline case since there is no filtration or inactivation of pathogens in the AHU for those cases. Thus, the two peaks correspond to the shoulder seasons (higher outdoor air usage) and hot or cold seasons (lower outdoor air usage). The two peaks for the HVAC system measures are dependent on the total airflow since they can provide higher equivalent clean air regardless of the outdoor air usage or because the outdoor airflow is already maximized for the max OA case. In this case, the two peaks correspond to the warmer months (higher total airflow to provide enough cooling) and colder or shoulder months (lower total airflow during heating mode or when less cooling is required). The distributions also often tail upwards because of occasional high airflows when the system turns on in the morning, especially when heat builds up overnight in the summer.

The MERV 8 baseline case meets the ASHRAE 241 clean air standard 74% of the time during occupied hours and never meets the CDC standard. The other measures always

meet the ASHRAE 241 standard. The HVAC system measures cannot meet the CDC target despite increasing the zone airflow setpoints to their maximum. This is because the standard size of the prototypical office building system in this study is unable to provide enough airflow to meet the CDC target in all the zones simultaneously. For other buildings, especially those with over-sized HVAC systems, meeting the CDC clean air target can be more feasible. Conversely, the in-room measures can meet the CDC clean air target in this study because they are not limited by how much airflow is supplied to the zones. In other words, the UR/WR GUV and PACs can be feasibly designed to meet the CDC target with the normal operation of the HVAC system.

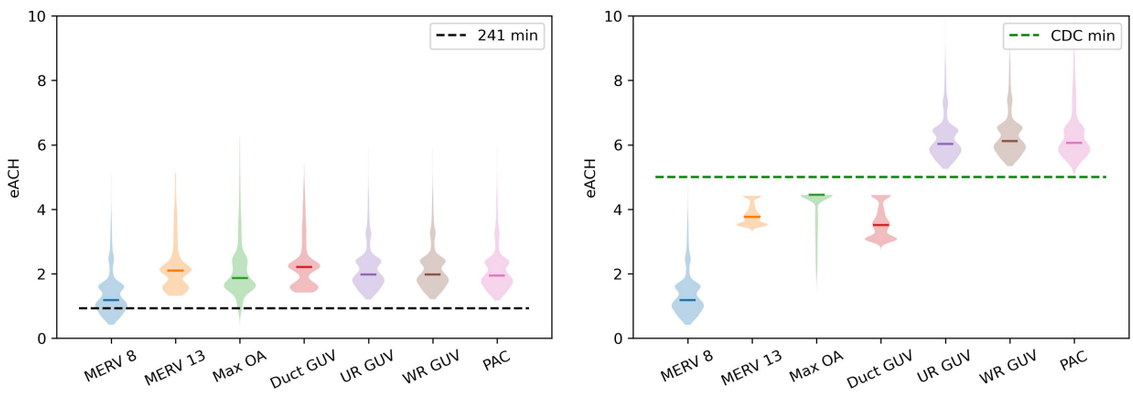

(a) ASHRAE 241.

(b) CDC.

Figure 3: Hourly distribution of eACH in the South zone for the two clean air targets. The horizontal, darker bars represent the median values.

Table 4 compares the MERV 8 eACH results in the South zone for two values of filtration efficiency: 0% based on ASHRAE 241 and 34% calculated using values from ASHRAE 52.2. The higher efficiency value increases the median eACH by 36% and results in the system meeting the ASHRAE 241 minimum 97% of the time compared to 74%. The system never meets the CDC target for either efficiency value.

Table 4: Comparison of MERV 8 eACH results in the South zone for two filtration efficiencies.

MERV 8 efficiency value	*Median eACH*	*Time meeting ASHRAE 241 minimum*	*Time meeting CDC target*
0%	1.2	74%	0%
34%	1.6	97%	0%

5.1.2. Energy-based Results

Next, Figure 4 shows the total annual energy consumption and Table 5 shows the annual CO_2 emissions for the scenarios. This assumes IRMM is in place for an entire year. The energy consumption does not increase significantly for the ASHRAE 241 cases compared to the baseline, except for the max OA case. This is because significant heating/cooling energy is needed to condition the higher amount of outdoor air. This study is applied for a cool and humid climate, so this increase in energy can be smaller for a milder climate or more significant for a climate with more extreme weather conditions. There are larger increases in energy for the HVAC system measures to meet the CDC target as well. This is because of high increases in fan energy to supply enough airflow to attempt to meet the CDC clean air target, which is not needed for the ASHRAE 241 cases. This increase in energy depends on the system sizing and may be less severe depending on the system design. The energy increases between the CDC and ASHRAE 241 cases are much smaller for the in-room measures, because these devices do not consume as much power and the operation of the HVAC system does not need to be modified. The emissions and energy trends align closely because the emission factors for gas and electricity are more similar for the studied location (Chicago, IL). They can deviate more when the electricity and gas emission factors differ greatly, for example in locations that use more renewable energy for electricity generation.

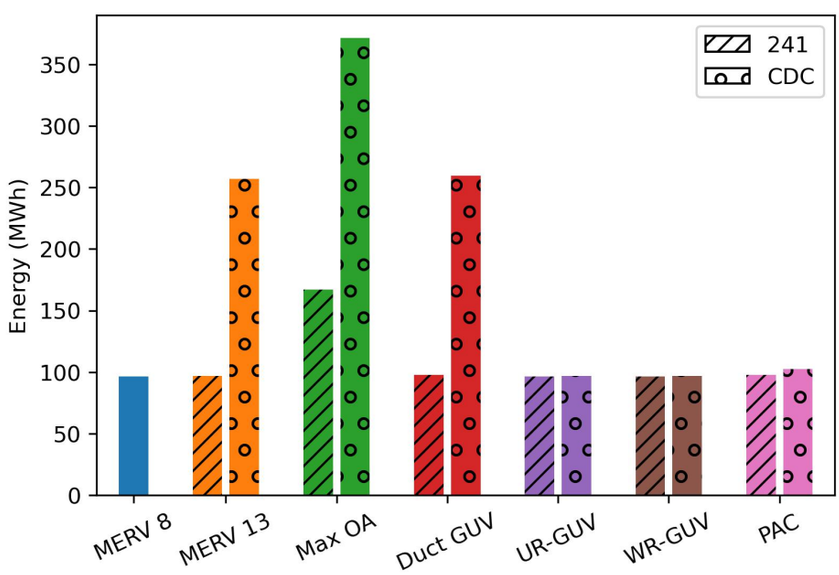

Figure 4: Total annual energy consumption for the mitigation measures to meet the two clean air targets.

Table 5: Annual CO_2 emissions for the measures to meet the two clean air targets.

Mitigation measure	*CO_2 emissions (kg)*	
	ASHRAE 241	*CDC*
MERV 8	21,887 (baseline)	
MERV 13	21,956	55,211
Max OA	35,378	76,980
Duct GUV	22,190	55,785
UR GUV	21,902	21,965
WR GUV	21,919	22,055
PAC	22,368	24,677

The total monthly energy consumption for the mitigation measures to meet the clean air guidelines is shown in Figure 5. This data is relevant to assess the impacts of implementing IRMM during different times of the year, for example during the winter months when infection risk may be higher. First, the most energy is consumed by this building during the winter because of the cold climate. Increasing the outdoor air usage to meet the ASHRAE 241 standard leads to a large energy increase during this time compared to a smaller increase during the summer and almost no change in the shoulder seasons. The increase in energy for the MERV 13 and duct GUV cases to meet the CDC target is more consistent throughout the year because the higher energy is a result of increased fan energy to provide enough total airflow to the zones to meet the target. Interestingly, the PAC case to meet the CDC target can consume less energy than the baseline during the colder months but more during the warmer months, because the power consumed by the PACs is modeled to be completely dissipated as heat into the rooms, so this lessens the heating demand during the colder seasons but increases the cooling demand during the warmer seasons.

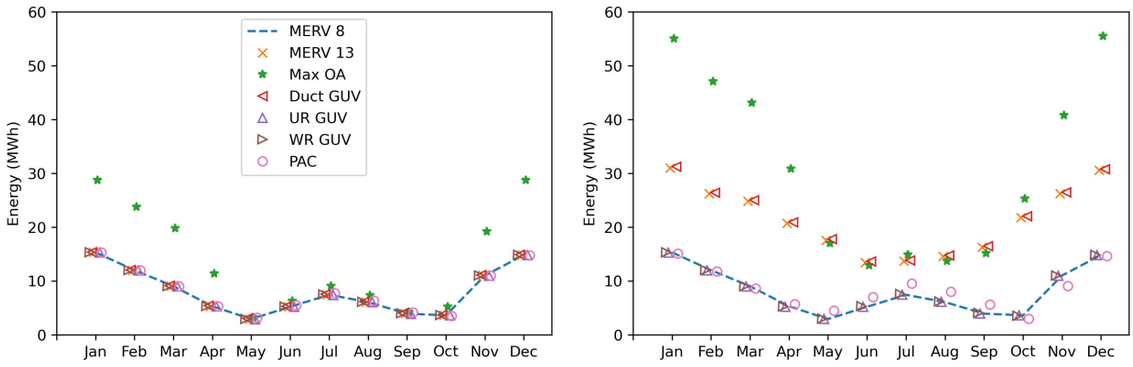

(a) ASHRAE 241.

(b) CDC.

Figure 5: Total monthly energy consumption for the mitigation measures to meet the two clean air targets.

The hourly distributions of energy consumption per eACH of the entire floor are shown for the different measures in Figure 6. Their median values are represented by the darker, horizontal bars and are also included in Table 6 along with the median incremental increase in energy per eACH, which are calculated as described in Section 4.1.2. The energy per eACH is similar for the ASHRAE 241 cases, except for the max OA case which consumes the most energy. The MERV 13 and duct GUV cases can have lower energy per eACH for these cases by providing very high eACH in an energy-efficient manner when the total supply airflow is high for all scenarios in the warmer months. However, the increase in fan energy throughout the year to supply enough airflow for these cases to meet the CDC target results in a higher average energy usage per eACH. Conversely, the in-room measures can increase their eACH in a much more energy efficient manner compared to ventilation, resulting in very low energy per eACH values for these cases to meet the CDC target. As a result, the median energy consumption per eACH can be up to 80% lower for the in-room measures compared to the HVAC system measures for the CDC cases.

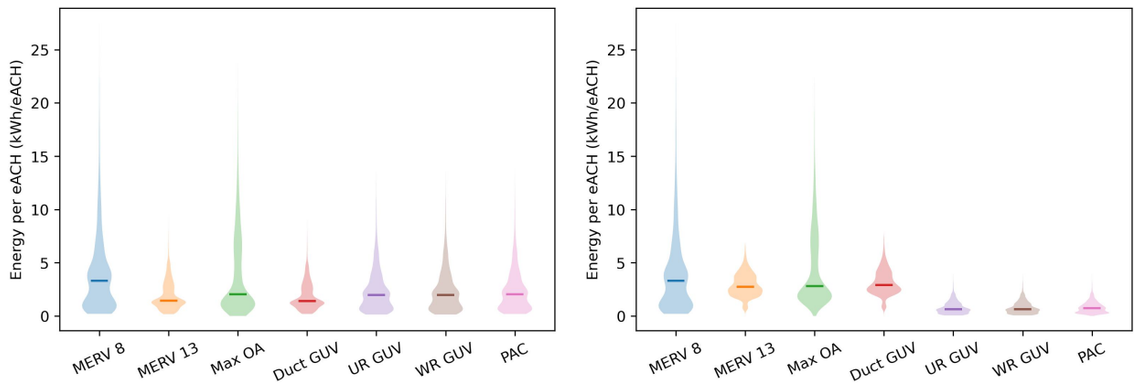

(a) ASHRAE 241.

(b) CDC.

Figure 6: Hourly distribution of energy consumption per eACH of the entire floor for the two clean air targets. The horizontal, darker bars represent the median values.

Table 6: Median values of hourly energy consumption per eACH and incremental increase in energy per eACH relative to the MERV 8 case for the mitigation measures.

Mitigation measure	*Energy per eACH (kWh/eACH)*		*Δ Energy / Δ eACH*	
	ASHRAE 241	*CDC*	*ASHRAE 241*	*CDC*
MERV 8	3.3		N/A	
MERV 13	1.4	2.7	0.002	0.7
Max OA	2.0	2.8	0.9	1.4
Duct GUV	1.4	2.9	0.006	0.8
UR GUV	2.0	0.6	0.001	0.001
WR GUV	2.0	0.6	0.003	0.003
PAC	2.0	0.7	0.05	0.05

5.1.3. Discomfort Results

Next, the annual temperature and humidity discomfort values in the South zone are shown in Table 7. First, there is some temperature and humidity discomfort for the baseline case because the system may take time to meet the temperature setpoint, especially when the setpoint changes once occupants arrive in the morning. The temperature and humidity discomfort is similar for the ASHRAE 241 cases, except the max OA case. This is because it becomes difficult to control the outdoor air usage to provide clean air while maintaining comfort for this case. This is exacerbated for the CDC case when the total airflow is also

increased. Interestingly, the MERV 13 and duct GUV cases reduce the discomfort for the CDC scenarios. This is because increasing the total airflow for these cases often results in over-cooling of the zones during the warmer months, which prevents occasional times of discomfort due to temperatures exceeding the cooling setpoint. Temperature and humidity heat maps are included in Appendix B to show these trends.

Table 7: Temperature and humidity discomfort in the South zone for the mitigation measures to meet the two clean air targets.

Mitigation measure	*Temperature Discomfort* ($°C \cdot hr$)		*Humidity Discomfort* ($°C \cdot hr$)	
	ASHRAE 241	*CDC*	*ASHRAE 241*	*CDC*
MERV 8	131 (baseline)		64 (baseline)	
MERV 13	132	75	64	31
Max OA	533	268	805	1226
Duct GUV	132	78	64	32
UR GUV	132	131	64	64
WR GUV	131	131	64	64
PAC	131	141	64	65

5.2. Detailed Analysis

Figure 7 shows the dynamic eACH results in the South zone during three representative days across different seasons: August 28 (summer), December 26 (winter), and May 1 (spring). The results show the HVAC system measures have higher eACH values during the summer day for the ASHRAE 241 standard. This is because they supply a high amount of equivalent clean airflow during this time while the total airflow is also high. On the other hand, while the total airflow is also high for the baseline and in-room cases, the equivalent clean airflow is not as high because the outdoor air fraction is lower during this time and there is no additional cleaning of the supply airflow. All of the measures tend to have lower eACH values for the ASHRAE 241 standard during the winter day because of the low total airflow and low outdoor air usage. Lastly, the in-room measures can have higher eACH values for the ASHRAE 241 standard during the spring day, because all of the cases use similar levels of high outdoor airflow for economizing on this day. As a result, all of the cases

have similarly high $eACH_{HVAC}$ values, but the in-room cases benefit from the additional eACH provided by the in-room devices.

The seasonal effects are slightly different for the CDC cases. Since the MERV 13 and duct GUV measures provide similar levels of total airflow throughout the year for these cases, they become more sensitive to the outdoor air usage. For example, their eACH values are highest during the spring day. The max OA case shows a different pattern for the winter day compared to the other days, because the fraction of outdoor air is reduced in the winter months to prevent freezing of the coils. The in-room measures show similar sensitivities to the outdoor air usage for the CDC cases compared to the ASHRAE 241 cases.

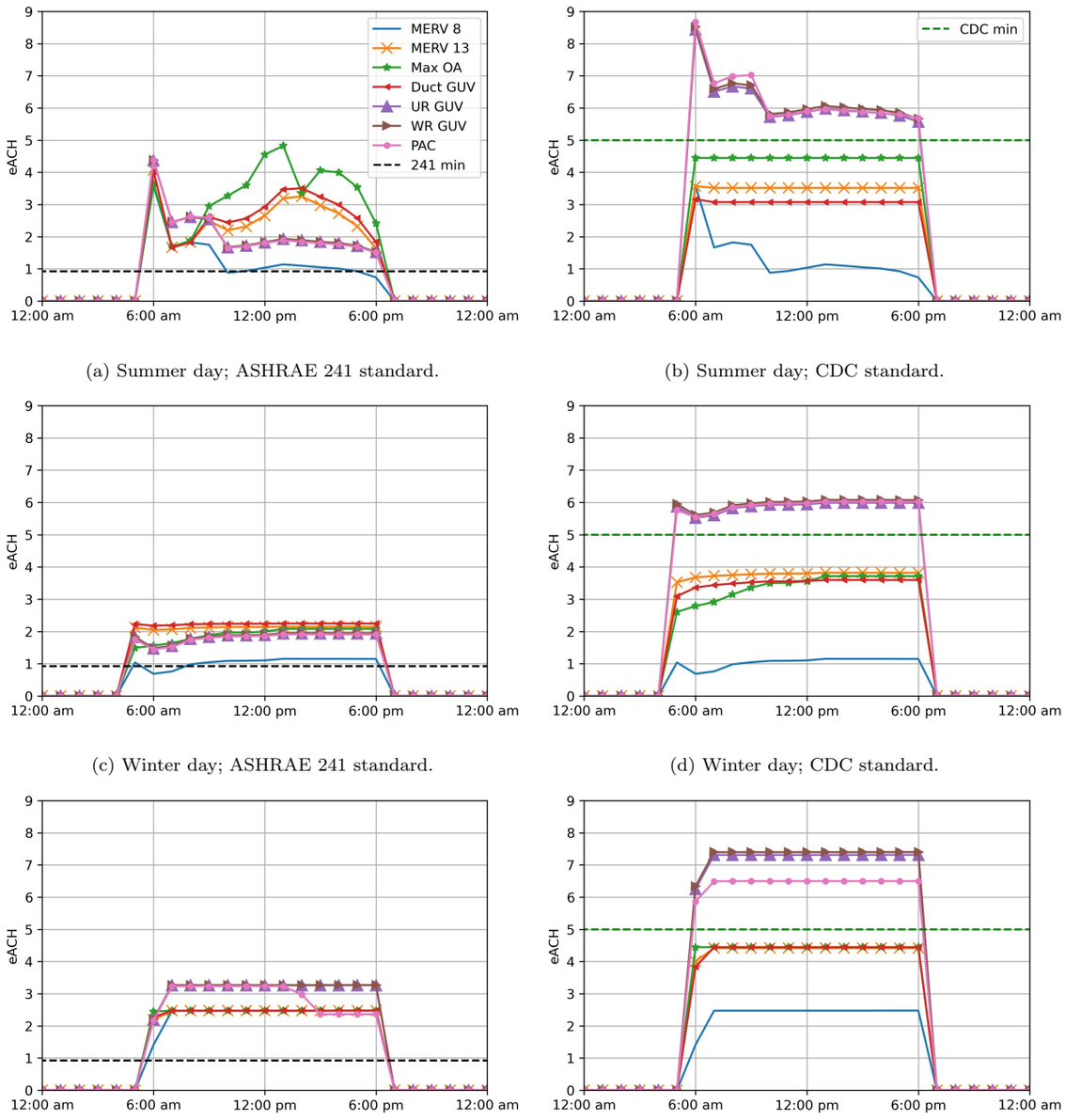

(a) Summer day; ASHRAE 241 standard.

(b) Summer day; CDC standard.

(c) Winter day; ASHRAE 241 standard.

(d) Winter day; CDC standard.

(e) Spring day; ASHRAE 241 standard.

(f) Spring day; CDC standard.

Figure 7: Plots of dynamic equivalent clean air changes per hour in the South zone for the two clean air target cases during three representative days.

5.3. Limitations of This Work

The following limitations exist for this study. First, the simulations were conducted for an office building in one climate, so the findings in this paper may be different for other buildings and climates. For example, the increase in energy for the maximum outdoor air case is strongly correlated with the climate and the ability of the HVAC system measures to meet the CDC target is dependent on the HVAC system design. ASHRAE Standard 241 also recommends different equivalent clean air targets depending on the space type. An infection risk analysis was not performed in this study, but the models used in this paper can be used to quantify infection risk for the different measures. A range of quanta emission rates and infector locations can be used to perform a detailed infection risk analysis when designing the measures to meet the clean air targets. This also allows for comparisons between eACH and infection risk, which can lead to interesting results since eACH does not depend on parameters such as the location in the building or strength of the pathogen source while infection risk is significantly impacted by those parameters. This study also assumes each zone is instantaneously and perfectly mixed (i.e., uniform temperature and concentration in each zone), which introduces a degree of uncertainty in the results [63] because aspects such as the location of the occupants, imperfect mixing, localized airflow patterns caused by the PACs, and more, are not modeled. Lastly, this study used the building design occupancy to determine the ASHRAE 241 clean air target during IRMM, but occupancy may be reduced during IRMM (e.g., increased remote workers for an office building), which would lower the clean air target.

6. Conclusion

This paper analyzed airborne pathogen mitigation measures including increased outdoor air ventilation, use of HVAC filtration or in-duct GUV, or application of GUV or PAC devices in rooms. The measures were designed to meet ASHRAE standard 241 and CDC clean air targets for one floor of a prototypical office building in a cool and humid climate. To support these analyses, new models were developed for GUV and PAC devices using Modelica language. The simulation scenarios were compared using a variety of metrics including eACH, energy consumption, CO_2 emissions, and thermal discomfort. The simulations were

conducted assuming IRMM operation for an entire year and the results were analyzed for annual, monthly, and daily temporal scales.

The results showed the various measures can meet the ASHRAE 241 standard for this office building without significant impacts on energy consumption and discomfort, except for the max OA case. The max OA case resulted in significant increases in energy consumption as well as high indoor temperatures and humidity during the peak of summer. Since maintaining comfort in buildings is a primary consideration, the results suggest increasing outdoor air ventilation should be done cautiously to avoid causing discomfort. The HVAC system measures were not able to meet the CDC clean air target because the system is not sized to deliver enough total airflow to the zones simultaneously in order to meet this target. Increasing the supply airflow to its maximum also resulted in significant energy penalties because of the increase in fan energy. However, the in-room GUV and PACs were able to meet the CDC target by directly cleaning the air in the room without the need to increase the airflow supplied to the zones. The energy consumption also did not increase significantly for these cases and the median energy consumption per eACH was up to 80% lower for the in-room measures compared to the HVAC system measures for the CDC cases.

The developed models and methods in this paper support future analyses. First, this study focused on a prototypical office building, but eACH standard for ASHRAE 241 can differ significantly depending on space type. For example, it can be higher than the CDC target for space types such as dining areas in restaurants. Future work can study the design of these measures to meet the clean air targets for different building types. Additionally, this study only considered one climate, but the impacts of ventilation or other measures can vary greatly across different climates. The CO_2 emission factor also depends on location, so future work can apply this methodology to multiple climates. Finally, this study focuses on applying measures to mitigate indoor airborne pathogens, specifically SARS-CoV-2. However, the studied measures have differing impacts when considering other pathogens or contaminants. For example, GUV is not effective against particulates such as smoke and filtration is not effective for gases such as CO_2. Future work can holistically study the measures for multiple contaminant scenarios and consider other pathogens to provide practical guidance to building operators for improving indoor air quality.

Acknowledgements

This work was supported by the DOE Building Technologies Office (BTO) within the Office of Energy Efficiency and Renewable Energy (EERE).

Appendix A: Verification of New Models for Air-Cleaning Technologies

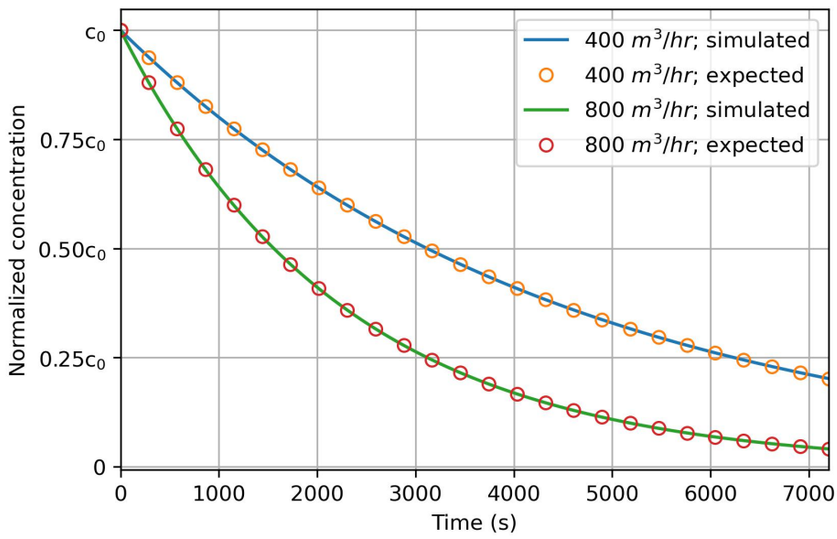

Figure A1: Verification of PAC model for a 500 m^3 room with an initial pathogen concentration of c_0 and without generation or removal of pathogens other than removal by PACs for two PAC flow rates: 400 m^3/hr and 800 m^3/hr.

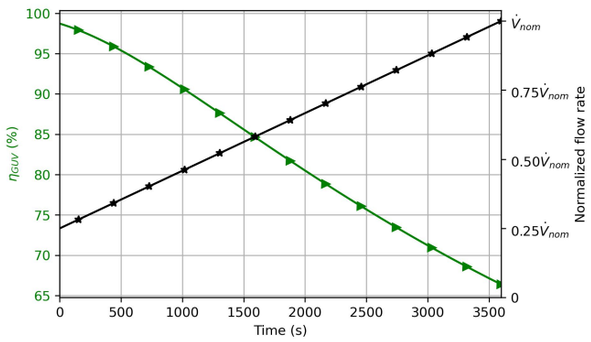

(a) In-duct GUV inactivation efficiency with varying flow rate.

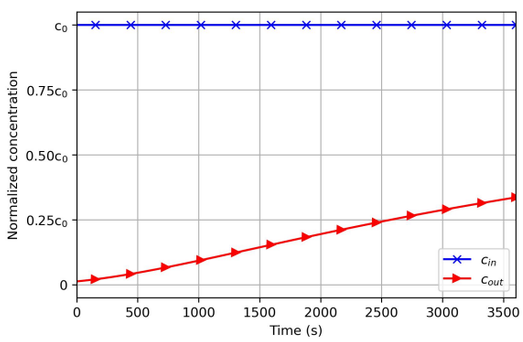

(b) Concentration in the flow through the in-duct GUV.

Figure A2: Demonstration of in-duct GUV pathogen inactivation as a function of flow rate using a k_{GUV} value of 1.09 and flow rate varying linearly from 25% of $\dot{V}_{nom}$ up to $\dot{V}_{nom}$. The pathogen concentration in the flow entering the irradiated volume of the in-duct GUV (c_{in}) is a constant value of c_0. The pathogen concentration in the flow exiting the irradiated volume of the in-duct GUV (c_{out}) depends on η_{GUV}, as expected based on Equations 3-5.

Appendix B: Temperature and Humidity Results

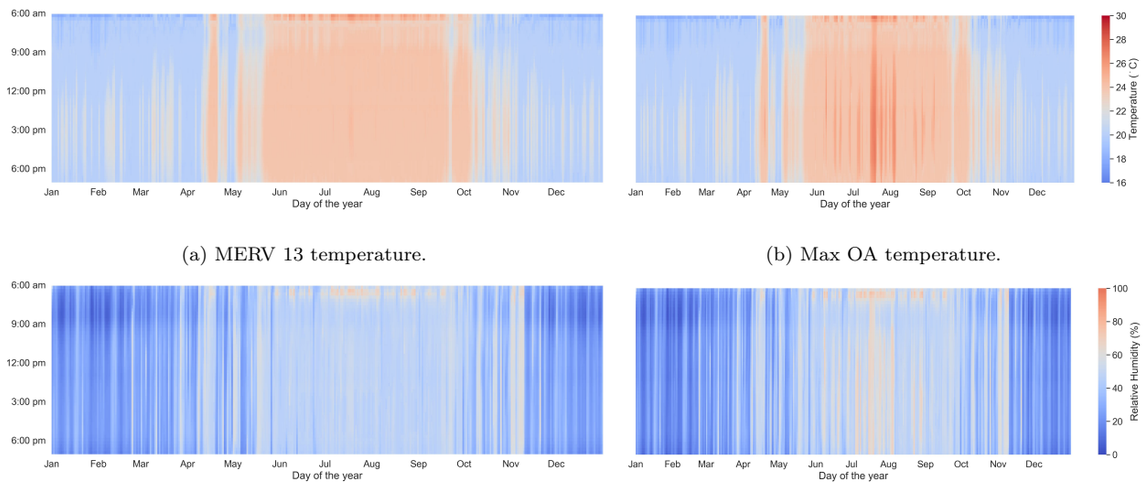

(a) MERV 13 temperature.

(b) Max OA temperature.

(c) MERV 13 humidity.

(d) Max OA humidity.

Figure B1: Temperature and humidity heat maps in the South zone for the MERV 13 and Max OA scenarios to meet the ASHRAE 241 standard.

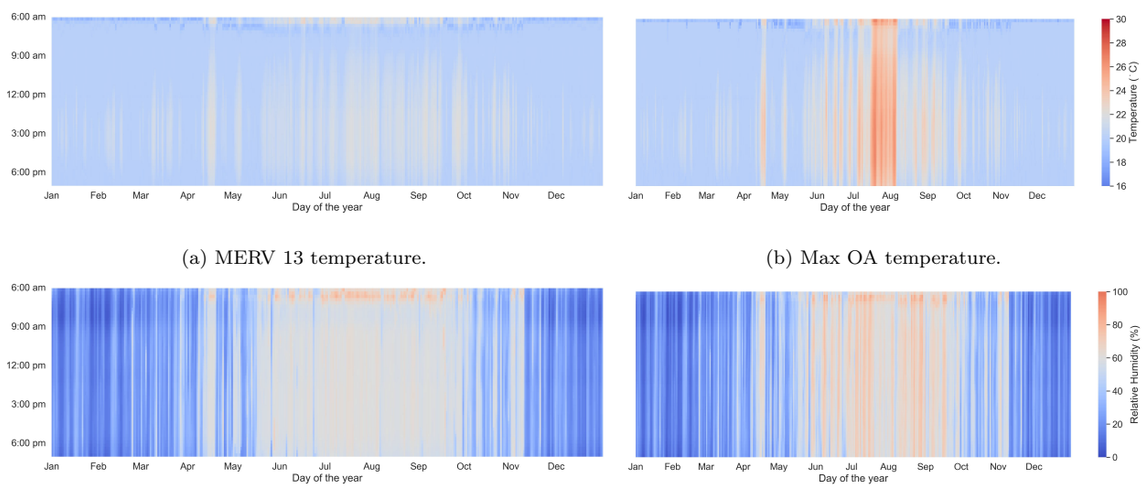

(a) MERV 13 temperature.

(b) Max OA temperature.

(c) MERV 13 humidity.

(d) Max OA humidity.

Figure B2: Temperature and humidity heat maps in the South zone for the MERV 13 and Max OA scenarios to meet the CDC target.

References

[1] H. Qian, T. Miao, L. Liu, X. Zheng, D. Luo, Y. Li, Indoor transmission of SARS-CoV-2, Indoor Air 31 (3) (2021) 639–645.

[2] S. L. Miller, W. W. Nazaroff, J. L. Jimenez, A. Boerstra, G. Buonanno, S. J. Dancer, J. Kurnitski, L. C. Marr, L. Morawska, C. Noakes, Transmission of SARS-CoV-2 by inhalation of respiratory aerosol in the Skagit Valley Chorale superspreading event, Indoor Air 31 (2) (2021) 314–323.

[3] L. Andrup, K.-A. Krogfelt, K.-S. Hansen, A.-M. Madsen, Transmission route of rhinovirus-the causative agent for common cold. A systematic review, American Journal of Infection Control (2022).

[4] L. Santibañez, C. M. Guarino, The effects of absenteeism on academic and social-emotional outcomes: Lessons for COVID-19, Educational Researcher 50 (6) (2021) 392–400.

[5] K. A. Gee, V. Asmundson, T. Vang, Educational impacts of the COVID-19 pandemic in the United States: Inequities by race, ethnicity, and socioeconomic status, Current Opinion in Psychology 52 (2023) 101643.

[6] G. S. Goda, E. J. Soltas, The impacts of COVID-19 absences on workers, Journal of Public Economics 222 (2023) 104889.

[7] A. Faramarzi, J. Javan-Noughabi, S. S. Tabatabaee, A. A. Najafpoor, A. Rezapour, The lost productivity cost of absenteeism due to COVID-19 in health care workers in Iran: a case study in the hospitals of Mashhad University of Medical Sciences, BMC health services research 21 (2021) 1–7.

[8] Center for Disease Control and Prevention, Ventilation in Buildings, https://www.cdc.gov/coronavirus/2019-ncov/community/ventilation.html (2023).

[9] ASHRAE, Standard 241 Control of Infectious Aerosols, American Society of Heating, Refrigerating and Air-Conditioning Engineers (2023).

[10] H. Y. Kek, S. B. M. Saupi, H. Tan, M. H. D. Othman, B. B. Nyakuma, P. S. Goh, W. A. H. Altowayti, A. Qaid, N. H. A. Wahab, C. H. Lee, et al., Ventilation Strategies for Mitigating Airborne Infection in Healthcare Facilities: A Review and Bibliometric Analysis (1993 to 2022), Energy and Buildings (2023) 113323.

[11] S. Ferrari, T. Blázquez, R. Cardelli, G. Puglisi, R. Suárez, L. Mazzarella, Ventilation strategies to reduce airborne transmission of viruses in classrooms: A systematic review of scientific literature, Building and Environment (2022) 109366.

[12] Z. Pang, X. Lu, Z. O'Neill, Quantification of how mechanical ventilation influences the airborne infection risk of covid-19 and hvac energy consumption in office buildings, Building Simulation 16 (5) (2023) 713–732.

[13] P. Azimi, B. Stephens, HVAC filtration for controlling infectious airborne disease transmission in indoor environments: Predicting risk reductions and operational costs, Building and Environment 70 (2013) 150–160.

[14] M. Zaatari, A. Goel, J. Maser, Why Equivalent Clean Airflow Doesn't Have To Be Expensive, ASHRAE Journal 65 (9) (2023) 18–24.

[15] M. J. Risbeck, A. E. Cohen, J. D. Douglas, Z. Jiang, C. Fanone, K. Bowes, J. Doughty, M. Turnbull, L. DiBerardinis, Y. M. Lee, M. Z. Bazant, Data-driven control of airborne infection risk and energy use in buildings, Building and Environment 245 (2023) 110893.

[16] ASHRAE, Standard 62.1 Ventilation for Acceptable Indoor Air Quality, American Society of Heating, Refrigerating and Air-Conditioning Engineers (2022).

[17] M. Buonanno, D. Welch, I. Shuryak, D. J. Brenner, Far-UVC light (222 nm) efficiently and safely inactivates airborne human coronaviruses, Scientific Reports 10 (1) (2020) 1–8.

[18] E. R. Blatchley III, B. Petri, W. Sun, SARS-CoV-2 ultraviolet radiation dose-response behavior, Journal of Research of the National Institute of Standards and Technology 126 (2021) 1–11.

[19] M. A. Schuit, T. C. Larason, M. L. Krause, B. M. Green, B. P. Holland, S. P. Wood, S. Grantham, Y. Zong, C. J. Zarobila, D. L. Freeburger, et al., SARS-CoV-2 inactivation by ultraviolet radiation and visible light is dependent on wavelength and sample matrix, Journal of Photochemistry and Photobiology B: Biology 233 (2022) 112503.

[20] E. R. Blatchley III, D. J. Brenner, H. Claus, T. E. Cowan, K. G. Linden, Y. Liu, T. Mao, S.-J. Park, P. J. Piper, R. M. Simons, et al., Far UV-C radiation: An emerging tool for pandemic control, Critical Reviews in Environmental Science and Technology 53 (6) (2023) 733–753.

[21] S. Yan, L. L. Wang, M. J. Birnkrant, J. Zhai, S. L. Miller, Evaluating SARS-CoV-2 airborne quanta transmission and exposure risk in a mechanically ventilated multizone office building, Building and Environment 219 (2022) 109184.

[22] S. Yan, L. Wang, M. J. Birnkrant, Z. Zhai, S. L. Miller, Multizone Modeling of Airborne SARS-CoV-2 Quanta Transmission and Infection Mitigation Strategies in Office, Hotel, Retail, and School Buildings, Buildings 13 (1) (2022) 102.

[23] S. Srivastava, X. Zhao, A. Manay, Q. Chen, Effective ventilation and air disinfection system for reducing coronavirus disease 2019 (COVID-19) infection risk in office buildings, Sustainable Cities and Society 75 (2021) 103408.

[24] H. Dai, B. Zhao, Reducing airborne infection risk of COVID-19 by locating air cleaners at proper positions indoor: Analysis with a simple model, Building and Environment 213 (2022) 108864.

[25] J. E. Castellini Jr, C. A. Faulkner, W. Zuo, D. M. Lorenzetti, M. D. Sohn, Assessing the use of portable air cleaners for reducing exposure to airborne diseases in a conference room with thermal stratification, Building and environment 207 (2022) 108441.

[26] B. Abboushi, G. Arnold, J. Tuenge, T. Salsbury, J. DeGraw, E. Nardell, Energy implications of using upper room germicidal ultraviolet radiation and HVAC strategies to combat SARS-CoV-2, Tech. rep. (2022).

[27] C. A. Faulkner, J. E. Castellini Jr, W. Zuo, D. M. Lorenzetti, M. D. Sohn, Investigation of HVAC operation strategies for office buildings during COVID-19 pandemic, Building and Environment 207 (2022) 108519.

[28] C. A. Faulkner, J. E. Castellini Jr, Y. Lou, W. Zuo, D. M. Lorenzetti, M. D. Sohn, Tradeoffs among indoor air quality, financial costs, and CO2 emissions for HVAC operation strategies to mitigate indoor virus in US office buildings, Building and Environment 221 (2022) 109282.

[29] C. A. Faulkner, J. E. Castellini Jr, W. Zuo, M. D. Sohn, Comprehensive analysis of model parameter uncertainty influence on evaluation of HVAC operation to mitigate

indoor virus: A case study for an office building in a cold and dry climate, Building and Environment 238 (2023) 110314.

[30] P. Fritzson, V. Engelson, Modelica—A unified object-oriented language for system modeling and simulation, in: ECOOP'98—Object-Oriented Programming: 12th European Conference Brussels, Belgium, July 20–24, 1998 Proceedings 12, Springer, 1998, pp. 67–90.

[31] Environmental Protection Agency, Overview of the Clean Air Act and Air Pollution, https://www.epa.gov/clean-air-act-overview (2023).

[32] Center for Disease Control and Prevention, Guidelines for Environmental Infection Control in Health-Care Facilities, https://www.cdc.gov/infectioncontrol/guidelines/environmental/appendix/air.html (2003).

[33] L. F. Pease, N. Wang, T. I. Salsbury, R. M. Underhill, J. E. Flaherty, A. Vlachokostas, G. Kulkarni, D. P. James, Investigation of potential aerosol transmission and infectivity of SARS-CoV-2 through central ventilation systems, Building and Environment 197 (2021) 107633.

[34] Environmental Protection Agency, What is a MERV rating?, https://www.epa.gov/indoor-air-quality-iaq/what-merv-rating (2023).

[35] M. Zaatari, A. Novoselac, J. Siegel, The relationship between filter pressure drop, indoor air quality, and energy consumption in rooftop HVAC units, Building and Environment 73 (2014) 151–161.

[36] Y. Yang, H. Zhang, S. S. Nunayon, V. Chan, A. C. Lai, Disinfection efficacy of ultraviolet germicidal irradiation on airborne bacteria in ventilation ducts, Indoor Air 28 (6) (2018) 806–817.

[37] J. J. Whalen, Environmental control for tuberculosis; basic upper-room ultraviolet germicidal irradiation guidelines for healthcare settings guide (2009).

[38] W. Kowalski, Uvgi lamps and fixtures, in: Ultraviolet germicidal irradiation handbook: UVGI for air and surface disinfection, Springer science & business media, 2010, pp. 119–137.

[39] C. J. Noakes, M. A. I. Khan, C. A. Gilkeson, Modeling infection risk and energy use of upper-room ultraviolet germicidal irradiation systems in multi-room environments, Science and Technology for the Built Environment 21 (1) (2015) 99–111.

[40] Z. Peng, S. L. Miller, J. L. Jimenez, Model Evaluation of Secondary Chemistry due to Disinfection of Indoor Air with Germicidal Ultraviolet Lamps, Environmental Science & Technology Letters 10 (1) (2022) 6–13.

[41] C. Noakes, C. Beggs, P. Sleigh, Modelling the performance of upper room ultraviolet germicidal irradiation devices in ventilated rooms: comparison of analytical and CFD methods, Indoor and Built Environment 13 (6) (2004) 477–488.

[42] S. Park, R. Mistrick, D. Rim, Performance of upper-room ultraviolet germicidal irradiation (UVGI) system in learning environments: Effects of ventilation rate, UV fluence rate, and UV radiating volume, Sustainable Cities and Society 85 (2022) 104048.

[43] S. Zhu, T. Lin, L. Wang, E. A. Nardell, R. L. Vincent, J. Srebric, Ceiling impact on air disinfection performance of Upper-Room Germicidal Ultraviolet (UR-GUV), Building and Environment 224 (2022) 109530.

[44] J. Xiang, C.-H. Huang, E. Austin, J. Shirai, Y. Liu, E. Seto, Energy consumption of using HEPA-based portable air cleaner in residences: A monitoring study in Seattle, US, Energy and buildings 236 (2021) 110773.

[45] I. G. Fernández de Mera, C. Granda, F. Villanueva, M. Sánchez-Sánchez, A. Moraga-Fernández, C. Gortázar, J. de la Fuente, HEPA filters of portable air cleaners as a tool for the surveillance of SARS-CoV-2, Indoor air 32 (9) (2022) e13109.

[46] H. Qian, Y. Li, H. Sun, P. V. Nielsen, X. Huang, X. Zheng, Particle removal efficiency of the portable HEPA air cleaner in a simulated hospital ward, Building Simulation 3 (2010) 215–224.

[47] E. A. Nardell, Air disinfection for airborne infection control with a focus on COVID-19: why germicidal UV is essential, Photochemistry and Photobiology 97 (3) (2021) 493–497.

[48] M. Wetter, W. Zuo, T. S. Nouidui, X. Pang, Modelica buildings library, Journal of Building Performance Simulation 7 (4) (2014) 253–270.

[49] M. Wetter, M. Bonvini, T. S. Nouidui, W. Zuo, Modelica buildings library 2.0, in: Proc. of The 14th International Conference of the International Building Performance Simulation Association (Building Simulation 2015), Hyderabad, India, 2015.

[50] E.-J. Sarabia-Escriva, V.-M. Soto-Francés, J.-M. Pinazo-Ojer, Mathematical model based on the radiosity method for estimating the efficiency of in-duct UVGI systems, Science and Technology for the Built Environment 28 (9) (2022) 1255–1269.

[51] P. Gagnon, B. Cowiestoll, M. Schwarz, Cambium 2022 Data, National Renewable Energy Laboratory (2023).

[52] D. Blum, J. Arroyo, S. Huang, J. Drgoňa, F. Jorissen, H. T. Walnum, Y. Chen, K. Benne, D. Vrabie, M. Wetter, et al., Building optimization testing framework (BOPTEST) for simulation-based benchmarking of control strategies in buildings, Journal of Building Performance Simulation 14 (5) (2021) 586–610.

[53] C. A. Faulkner, R. Lutes, S. Huang, W. Zuo, D. Vrabie, Simulation-based assessment of ASHRAE Guideline 36, considering energy performance, indoor air quality, and control stability, Building and Environment 240 (2023) 110371.

[54] Department of Energy, Commercial Reference Buildings, https://www.energycodes.gov/prototype-building-models#Commercial.

[55] Lawrence Berkeley National Laboratory, Buildings.Examples.VAVReheat, https://simulationresearch.lbl.gov/modelica/releases/v5.0.0/help/Buildings_Examples_VAVReheat.html#Buildings.Examples.VAVReheat (2013).

[56] ASHRAE, Standard 52.2 Method of Testing General Ventilation Air-Cleaning Devices for Removal Efficiency by Particle Size, American Society of Heating, Refrigerating and Air-Conditioning Engineers (2017).

[57] Dwyer, MERV 8 Pleated Filters, https://dwyer-inst.com/PDF_files/Priced/DF8_cat.pdf.

[58] Dwyer, MERV 13 Pleated Filters, https://dwyer-inst.com/PDF_files/Priced/DF13_cat.pdf.

[59] H. Luo, L. Zhong, Ultraviolet germicidal irradiation (UVGI) for in-duct airborne bioaerosol disinfection: Review and analysis of design factors, Building and environment 197 (2021) 107852.

[60] American Conference of Governmental Industrial Hygienists, in: 2022 Threshold Limit Values (TLVs) and Biological Exposure Indices (BEIs), 2022.

[61] J. Karam, K. Ghali, N. Ghaddar, Pulsating jet ventilation add-ons performance for reducing the contaminant spread in classrooms: Portable air cleaners vs. upper room UVGI, Building and Environment 229 (2023) 109946.

[62] Environmental Protection Agency, What is a HEPA filter?, https://www.epa.gov/indoor-air-quality-iaq/what-hepa-filter (2023).

[63] J. E. Castellini Jr, C. A. Faulkner, W. Zuo, M. D. Sohn, Quantifying spatiotemporal variability in occupant exposure to an indoor airborne contaminant with an uncertain source location, Building Simulation 16 (6) (2023) 889–913.